ORIGINAL ARTICLE

Predicting the fate of BTEX pollution and evaluating the remediation efficiency in an industrial site

Abdorreza Vaezihir[1] · Mansoureh Mohammadzadeh Motlaq[1] · Shoaib Bakhtiari[1] · Zeinab Ahmadnezhad[1] · Mehri Tabarmayeh[1]

Abstract

This study focused on estimating the aquifer hydraulic parameters of Bandar Abbas Refinery in Iran through a pumping test and investigating the fate of detected oil pollution using numerical flow and contaminants transport simulation models, namely MODFLOW-2000 and MT3DMS. The hydraulic conductivity, transmissivity, and specific yield were estimated to be 2.45 m/day, 24.5 m^2/ day, and 0.174, respectively. The steady-state model indicated the most sensitivity to the hydraulic head boundary and was run with a Normalized Root Mean Square of 4.97%, while the transient model was characterized by high sensitivity to hydraulic conductivity and longitudinal dispersivity established with NRMS of 2.7 to 4.26%. The transport model was used to simulate the effects of five different remediation scenarios over a period for 30 and 50 years considering both continuous and non-continuous leakage, with and without sorption processes. In the worst-case scenario with continuous and no sorption, the mean pollution level is predicted to reach 247.5 after 30 years and 310 after 50 years. However, in the best-case scenario, which involves cutting off the pollution source, implementing sorption processes, and eliminating the LNAPL without continuous and no sorption, the anticipated pollution levels are 97.5 after 30 years and 132.5 after 50 years. In the realistic scenario, where pollution is removed up to 50% with active and non-continuous state, the mean pollution value will be changed to 112.5 and 162.5 over the given period, respectively. These findings indicate the positive effect of remediation strategies in preventing the spread of pollution downstream.

Highlights

- Determination of the BTEX source release into groundwater from a real refinery site.
- Simulating groundwater flow and contaminants transport using MODFLOW-2000 and MT3DMS.
- Evaluating remediation scenarios efficiency by numerical modeling.
- Prediction of BTEX transport in the aquifer under the condition of various remediation scenarios.

Introduction

Oil contamination is one of the main threats to groundwater pollution, especially in oil-producing countries. Oil contamination leaks from tanks, facilities, and pipelines into the unsaturated zone and may percolate to reach groundwater. Oil-free phase can be laid on the top of the water table or may be descend to reach the aquifer bottom according to relative density. If the relative density of oil material is less than water, they are named Light Non-Aqueous Phase Liquid (LNAPL) and if it is more than water density, they are named Dense Non-Aqueous Phase Liquid (DNAPL) (Ismail et al. 2023). Many oil products such as gasoline, kerosene, and gasoil are ranked as LNAPL, whereas tar and asphalt are known as DNAPLs. The NAPL phase of oil cannot be distributed in the aquifer medium, but the solved phased source from the NAPL phase is more mobile and can be transported to a far distance from the source in groundwater. Benzene, Toluene, Ethylbenzene, and Xylene (all belonging to the BTEX group) are more soluble and toxic oil materials

✉ Abdorreza Vaezihir
r.vaezi@tabrizu.ac.ir

1 Department of Earth Sciences, University of Tabriz, 29 Bahman Blvd, Tabriz 5166616471, Iran

that can cause health problems related to their concentration and the duration of exposure (Zanello et al. 2021).

When a contaminant has been detected in an abstraction source (well or spring) it means that the contamination has been distributed very far from the source and the remediation process will be much more expensive and time-consuming, therefore detection of the pollutant at the early time of leak is necessary. Also, the elimination of pollution from groundwater is very expensive and time-consuming. Any mistake in the prediction of contaminants transport may cause many costs in implementing a clean-up program. Therefore, it is necessary to design and install a groundwater monitoring network at an industrial site After monitoring the groundwater and detecting polluted wells, the second step is finding the source, then simulation of contaminant transport modeling can simulate pollution transport and prediction of its future spreading as well as evaluation of remediation operation (Anderson et al. 2015). Groundwater -modeling is an efficient way to understand the physical and chemical processes that govern the BTEX behavior. The protocol of a mathematical model involves describing the study area using laboratory and field observations, developing a conceptual model, inputting the data to the numerical model, and completing the running process by sensitivity analysis and calibration (Schirmer et al. 2000).

In many studies, NAPL dissolution, mobilization, and removal mechanisms have been investigated (Vaezihir et al. 2013; Babaei and Copty 2019; Badv et al. 2020; Ramezanzadeh et al. 2022). Also, several physical models (Cheng et al. 2016; Leili et al. 2017; Vaezihir et al. 2020; Ahmadnezhad et al. 2021), as well as many numerical transport models, are used to better understand and predict plume spreading and fate in groundwater (Valsala and Govindarajan 2018, 2019; Seyedpour et al. 2019; Teramoto and Chang 2020). Among the models used for plume simulation and NAPL behavior, BIOPLUME (Rifai, 1997), NAPL simulator (Guarnaccia 1997), BIOMOC (Essaid and Bekins 1997), and BIONAPL/3D (Molson 2017) can be mentioned with acceptable simulations. MODFLOW as the most famous groundwater flow modeling tool can be conjugated with other codes like MT3D (Sharma et al. 2015; Ayvaz 2016; Sathe and Mahanta 2019; Bai et al. 2019; Bedekar 2019) and MODPATH to produce a powerful graphic tool for prediction of plume distribution or shrinkage (Guiguer and Franz 1994). In addition, the distribution of dissolved hydrocarbon plumes has been evaluated in field tests (Vaezihir et al. 2012; Steiner et al. 2018; Rama et al. 2019; Wang 2020; Ciampi et al. 2021; Demenev et al. 2022) and refinery sites (Pal et al. 2016; Bayatian et al. 2018; Hamamin 2018; Feng et al. 2020). Consequently, effective clean-up strategies and scenarios have been designed and presented for the remediation of groundwater contaminated by petroleum (He et al. 2009; Srivastav et al. 2018; O'Connor et al. 2018; Palma et al. 2019; Ghosh et al. 2020; Shafieiyoun et al. 2020).

Despite the relatively recent establishment of the Bandar Abbas Oil Refinery (since 1997), several concerns about oil contamination in groundwater have been reported at the refinery site. This issue has been previously addressed in a study conducted by Vaezihir et al. (2021), by detecting the presence of Light Non-Aqueous Phase Liquid (LNAPL) in groundwater. These findings indicated the potential contamination of a variety of oil pollutants, including gasoline, crude oil, and high-viscosity phases such as fuel oil resulting from leaching in different operations at the refinery. However, the previously conducted study has not comprehensively identified the sources of contamination, nor has it effectively investigated the fate of the contamination. This research aims to seek this limitation by detecting the polluted areas and finding possible sources as well as predicting the movement of the plume in groundwater. Evaluating the effectiveness of various remediation scenarios through numerical modeling and estimating the hydraulic coefficient of the aquifer using a pumping test is other goals of this research.

The main point of conducting this study lies in its comprehensive approach to understanding and addressing the BTEX contamination realizing source in the groundwater and simulating plume behavior using finite difference MODFLOW and MT3D models to provide valuable insights into the future distribution of BTEX compounds. Furthermore, the prediction of BTEX transport under different remediation scenarios will contribute to the development of effective mitigation strategies. Conducting this study and addressing its limitations will make a significant contribution to enhance the understanding and management of groundwater contamination in industrial sites, ultimately leading to improved environmental protection and public health outcomes.

Study area

The Bandar Abbas oil refinery was established in 1997 on the seaside of the Persian Gulf, approximately 30 km from the city of Bandar Abbas (Fig. 1).

The average annual temperature of this area is 27 °C, characterized by a mild winter, and a hot humid summer, while the average annual precipitation recorded in the data series from 1982 to 2015 is 161.52 mm. According to climatology data from the Bandar Abbas Climatology Station, the climate of the area is classified as dry categorize using the De Martonne method (De Martonne 1926). The geological main formations found at the site include gray marl and clayey limestone of Mishan formation (Mn), conglomerate
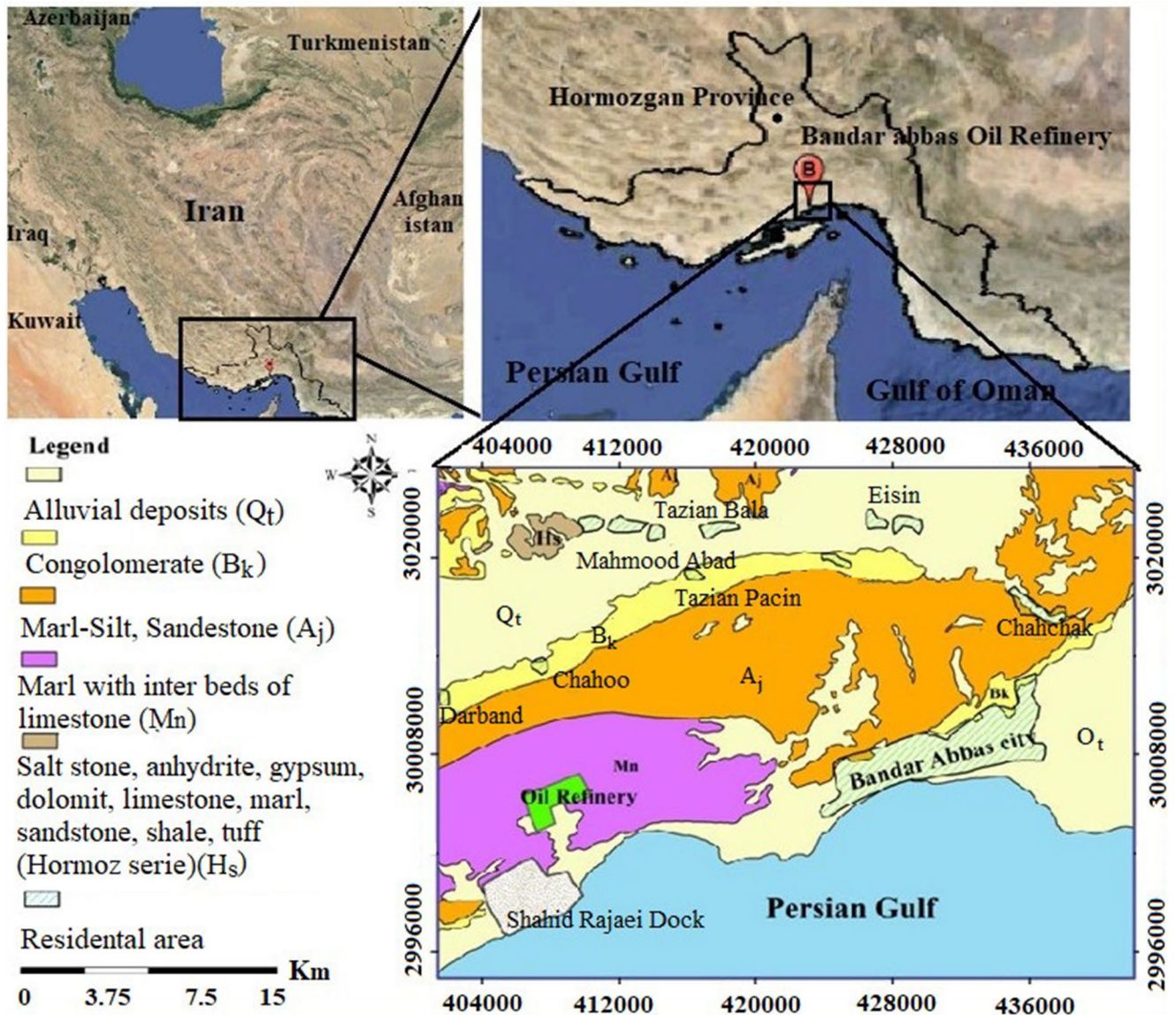
Fig. 1 Location and geology map of the study area. (Adapted from Map 1:100000 Geology of Bandar Abbas, National Iranian Oil Company 2010)

Bakhtiari formation (BK), and lime-bearing sandstone with layers of Marl and siltstone of the Aghajari formation (Aj) (Talbot and Alavi 1996). Another geological unit at the site is the Hormoz series with the Precambrian age. It is composed of colored salts with layers of dark dolomite- sandstone, and siltstone- marl. This geological unit is the main reason for the salinity of soil and water in the area (Talbot et al. 2009). Geophysics studies conducted by Leili et al. (2017) at the site and the cores obtained from geotechnical drilling have revealed that the aquifer of the refinery consists of alluvial sediments and weathered marl with an average thickness of 18 m.

Materials and methods

To monitor the groundwater levels, a total of 102 monitoring wells were used in this research. To evaluate the hydrochemistry and determine the type of groundwater, as well as detect any oil contaminants, 40 samples were collected from boreholes in different areas within the refinery in two sampling rounds in March 2017 and September 2018. A dedicated gradual sampling device was used for collecting samples, which was composed of a dead-end tube equipped with a valve and a small hole in the tube body. These samples were then sent to the central laboratory of the University of Tabriz for analysis. In-situ measurements were also conducted for parameters such as electrical conductivity (EC), pH, and temperatures. Samples were collected in each
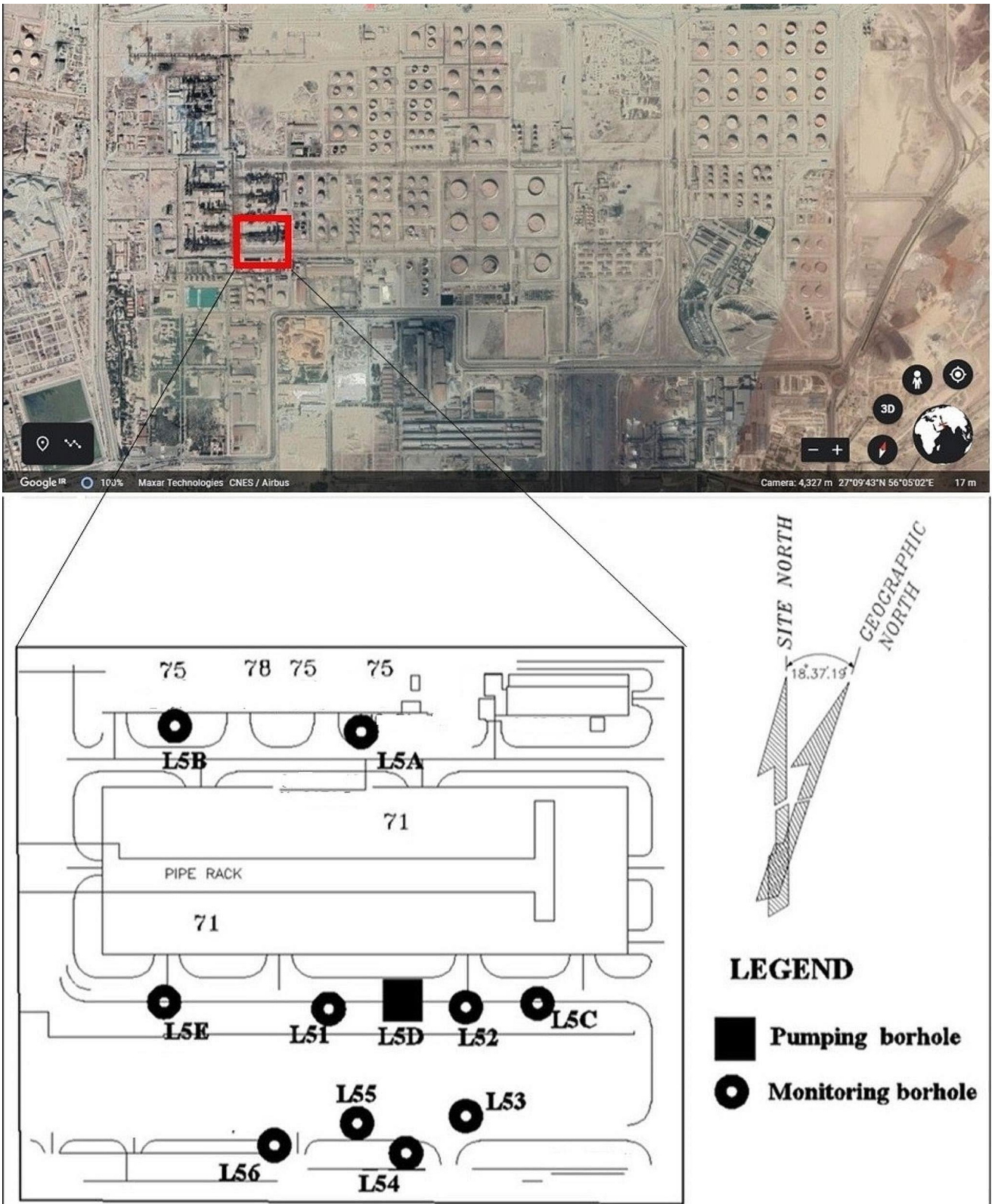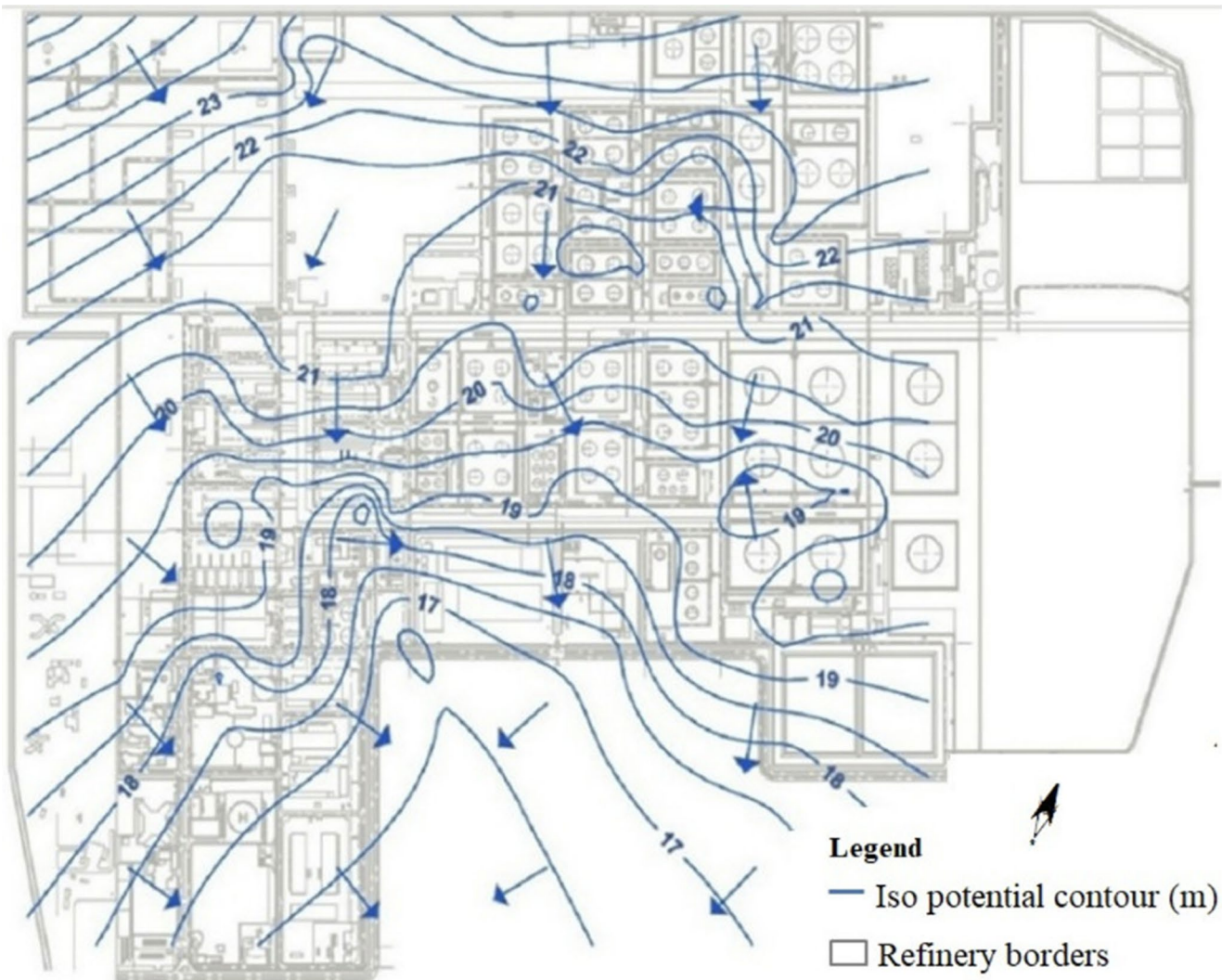
Fig. 2 Location of pumping and monitoring wells

borehole by a dedicated sampler to avoid cross-contamination and the amber glass vials were used with a sealed plastic cap. Analysis for hydrocarbon materials was carried out with a gas chromatography machine equipped with a

Fig. 3 Iso-potential water level map with contour lines in meters

mass spectrometry detector. The equipment model was GC Agilent 6890 N and MS Agilent 5973 N connected to a column with a length of 30 m and diameter of 0.25 mm with a carrier gas of helium.

For the extraction of samples in the lab, the micro-liquid method was employed, in which dichloromethane was used as a solvent in this extraction method. The purpose of this method was to transfer oil materials from water into the solvent phase, which is necessary for injection into the GC machine. To prepare the analyte, 3 ml of sample was mixed with dichloromethane and shaken for 10 h, and then the mixture was allowed to be kept in the refrigerator without shaking for 12 h (for the separation of two phases of water and solvent). Finally, 1 µL of it was injected into the GC machine inlet to analyze with a special temperature schedule. The schedule begins with an initial temperature of 40 ˚C, which is held for 30 s. Then the temperature was increased to 150 ˚C at a rate of 5 ˚C/ min and held in this temperature for 30 s. After that, the second increase

of temperature was done up to 290 ˚C and was held for 1 min. Analysis of other ions and compounds was carried out based on standard methods.

Aquifer Test

To determine the hydrodynamic parameters of the aquifer, a pumping test, also known as an aquifer test, was carried out in a well L5D. This well is adjacent to three monitoring wells: L51, L52, and L53. Wells L51 and L52 located at a distance of 15 m from the pumping well, while well L53 is situated 68 m away from it (Fig. 2).

The average discharge rate of the pumping during the aquifer test was 57.6 m³/d and the well diameter was 10 mm. The well was equipped with PVC pipe, which screened at the saturated part of the aquifer allowing for partial penetration of water into the aquifer (Table A.1 and Table A.2 in supplementary file). The test was continued for 6 h and the discharge of

the pumping well was measured hourly by a scaled tank. It is important to note that longer pumping tests are typically more effective in comprehensively understanding the properties and characteristics of an aquifer. However, due to limited options, it was not feasible to conduct a longer test in this particular study. To prevent groundwater recharge, the pumped water was conveyed to the recycling unit of the refinery instead of being discharged back into the aquifer. Then, drawdown-time data collected during the test are used to calculate the hydraulic characteristics of this unconfined aquifer by the Neumann-type curve (Neuman 1975).

Flow and transport modeling

Modeling and simulation of groundwater is a prerequisite for mass transport modeling. Therefore, it is necessary to calibrate aquifer and groundwater parameters in the flow modeling process, in which the results are used as inputs for the mass transport model. In this research, MODFLOW/2000 was employed to simulate the behavior of the groundwater. The selected area for flow modeling was a cubic rectangular volume with dimensions of 4500, 4000, and 10 m in length, width, and thickness, respectively.

The model area was discretized into 10,000 cells with a dimension of 40×40 m. However, in areas with a high density of monitoring wells, a telescoping discretization technique was employed to increase the accuracy and facilitate model convergence, resulting in a final network consisting of 18,480 cells and nodes. Groundwater flow direction was determined using water level data collected in March 2017 and the results were incorporated into the model (Fig. 3). To evaluate the weighted average groundwater level, the Thiessen Polygon method was used to dedicate areas to each monitoring well. The water table data revealed that in March 2017, the groundwater system was in a steady state condition. Therefore, this time was considered a steady state period for the first run of the model (See Fig. A.1 and Fig. A.2 in the supplementary file).

The total annual precipitation of the study area is approximately 164 mm, of which 34 mm was considered for a steady state period (March 2017). Of the total precipitation, 20% (6.8 mm) was assumed to percolate into groundwater. Since the evaporation from the groundwater table is influenced by the groundwater depth, a groundwater iso-depth map was prepared for the steady state period. The map indicated that a large portion of the site has a groundwater depth of less than 5 m, making it susceptible to evaporation (Fig. A.3 in supplementary file). Therefore, evaporation modules were activated during the modeling process. Bedrock depth was estimated to be in the range of 8 to 18 m and hydraulic conductivity, storage coefficient, and specific yield were estimated to be 2.45 m/d, 0.001, and 0.17, respectively.

These estimations were based on well drilling data and core logs.

According to the hydrological findings of the site, specific boundary conditions were assigned to each boundary in the groundwater model. The North and South boundaries were designated as general head boundary types, acting as inlet and outlet for the model, respectively. The East and west boundaries were also assigned as general head boundaries with low permeability. The bottom boundary was set as a no-flow boundary. The top boundary of the model was considered as a charge and discharge boundary, influenced by precipitation and evaporation. Additionally, an internal boundary was defined within the model to simulate drainage. This internal boundary, located in the middle of the modeling area, facilitates the representation of the drainage process (Fig. A.4 in supplementary file).

The water table data belongs to March 2017 as the steady period set as the initial value for the model. The stress period for running the model was defined as three months, corresponding to the duration from March 2017 to September 2017, and simulated on a daily basis. The time step for simulating the model was considered to be one day, allowing for the modeling of the water table in an unsteady state condition over this period (Fig. A.5 in supplementary file). The Successive Over-Relaxation (SOR) package was used to solve the model in the first attempt.

Results and discussion

According to the aquifer test results presented in Table 1, the hydraulic conductivity of the aquifer in the study area was calculated to be 2.45 m/d. The transmissivity and specific yield were determined to be 24.5 m²/d and 0.174 respectively. The estimated ratio of vertical to horizontal hydraulic conductivity (kv/kh), and specific yield to storage (SY/S) are to be 0.063 and 166, respectively (Table 2). However, the calculated hydraulic conductivity of 2.45 m/d is significantly higher than the typical values expected for marl aquifers, as suggested by Todd and Mays (2005) and Batu (2005), which typically fall between 0.08 m/d and $2 \times 10-4$ m/d. This discrepancy may result from the presence of fractures or solution conduits within the marlstone and limestone layers in the aquifer of Bandar Abbas Refinery. Regarding 2.45 m/d for hydraulic conductivity and 0.008 for hydraulic gradient (calculated from the iso potential map of groundwater), the average velocity of groundwater is estimated as 0.02 m/d.

Moreover, the monitoring of LNAPL phase thickness, in the 102 monitoring wells of the refinery revealed that 11 wells were contaminated by free phase oil with LNAPL thickness ranging from 2 cm in well L53 to 130 cm in well

Table 1 Drawdown-time data of aquifer test collected from the observation wells

L51			L52			L53		
Time (min)	Water level depth (m)	Drawdown (cm)	Time(min)	Water level depth (m)	Drawdown (cm)	Time (min)	Water level depth (m)	Drawdown (cm)
0	4.57	0	0	4.91	0	0	3.1	0
10	4.62	5	10	5.02	11	10	3.1	0
20	4.7	13	20	5.1	19	20	3.1	0
30	4.74	17	30	5.15	24	30	3.1	0
40	4.77	20	40	5.17	26	40	3.11	1
50	4.81	24	50	5.19	28	50	3.11	1
60	4.84	27	60	5.20	29.5	60	3.12	2
70	4.85	28	70	5.21	30.5	70	3.13	3
80	4.88	31	80	5.22	31.5	80	3.13	3
90	4.88	31	90	5.23	32	90	3.14	4
100	4.9	33	100	5.23	32.5	100	3.14	4
110	4.92	35	110	5.24	33	110	3.14	5
120	4.92	35	120	5.24	33	120	3.15	5
130	4.95	38	130	5.25	34	130	3.15	5
140	4.95	38	140	5.25	34	140	3.15	5
150	4.95	38	150	5.25	34.5	150	3.15	5
160	4.96	39	160	5.25	34.5	160	3.15	5
170	4.97	40	170	5.25	34.5	170	3.15	5
180	4.99	42	180	5.26	35	180	3.15	5
190	4.99	42	190	5.26	35	190	3.15	5
200	4.99	42	200	5.26	35	200	3.15	5
210	5	43	210	5.26	35	210	3.15	5
220	5	43	220	5.26	35	220	3.15	5
230	5.01	44	230	5.26	35.3	230	3.15	5
240	5.01	44	240	5.26	35.5	240	3.15	5
250	5.02	44	250	5.26	35.5	250	3.15	5

Table 2 Input parameters for transport modeling of each BTEX component

Contaminant Parameter	B	T	E	X	Source
density (Kg/m^3)	878.6	870	870	870	Wiedemeier et al. (1999)
Solubility in water (mg/L)	1780	515	152	198	Wiedemeier et al. (1999)
Distribution coefficient (K_d) (mg/L)	$10^{-7} \times 1.35$	$10^{-6} \times 1.23$	$10^{-7} \times 7.28$	$10^{-6} \times 1$	Calculated
Diffusion coefficient (m^2/d)	$10^{-5} \times 6.65$	$10^{-5} \times 5.7$	$10^{-5} \times 5.18$	$10^{-5} \times 4.83$	Calculated
Longitudinal dispersion (m)	10	10	10	10	Todd and Mays 2005
Lateral dispersion (m)	0.1	0.1	0.1	0.1	Todd and Mays 2005
Transverse dispersion (m)	0.05	0.05	0.05	0.05	Todd and Mays 2005
Initial concentration (mg/L)	0	0	0	0	Calculated

L5D. Furthermore, the results identified LNAPL mounds and their associated soluble plumes at the site. Among these mounds, mound 1, located in the south of refining unit 71, was selected to simulate the released plume. This plume was selected because of its specific characteristics, including (a) the maximum LNAPL thickness of 130 cm, (b) the proximately of this plume to the alluvial parts of the aquifer, which may increase the spread rate of the pollutants, (c) its separation from other plumes with no possible interface,

and (d) high confidence in detecting of the source. Besides, Mass labeled No. 2, No. 3, No. (4, 5, 7, 10), No. 6, No. 8, and 9 are located south of the recycling unit (Unit 26,002), south of Reservoir 200,006 (Crude Oil Reservoir), the south of the gasoline reservoirs, the south of Nafta Reservoir, and the south of A.T.K Reservoir, respectively. (Fig. 4).

Before developing the model, the leakage source for the plume, which needs to be assigned to the model as the starting point of plume distribution was determined.
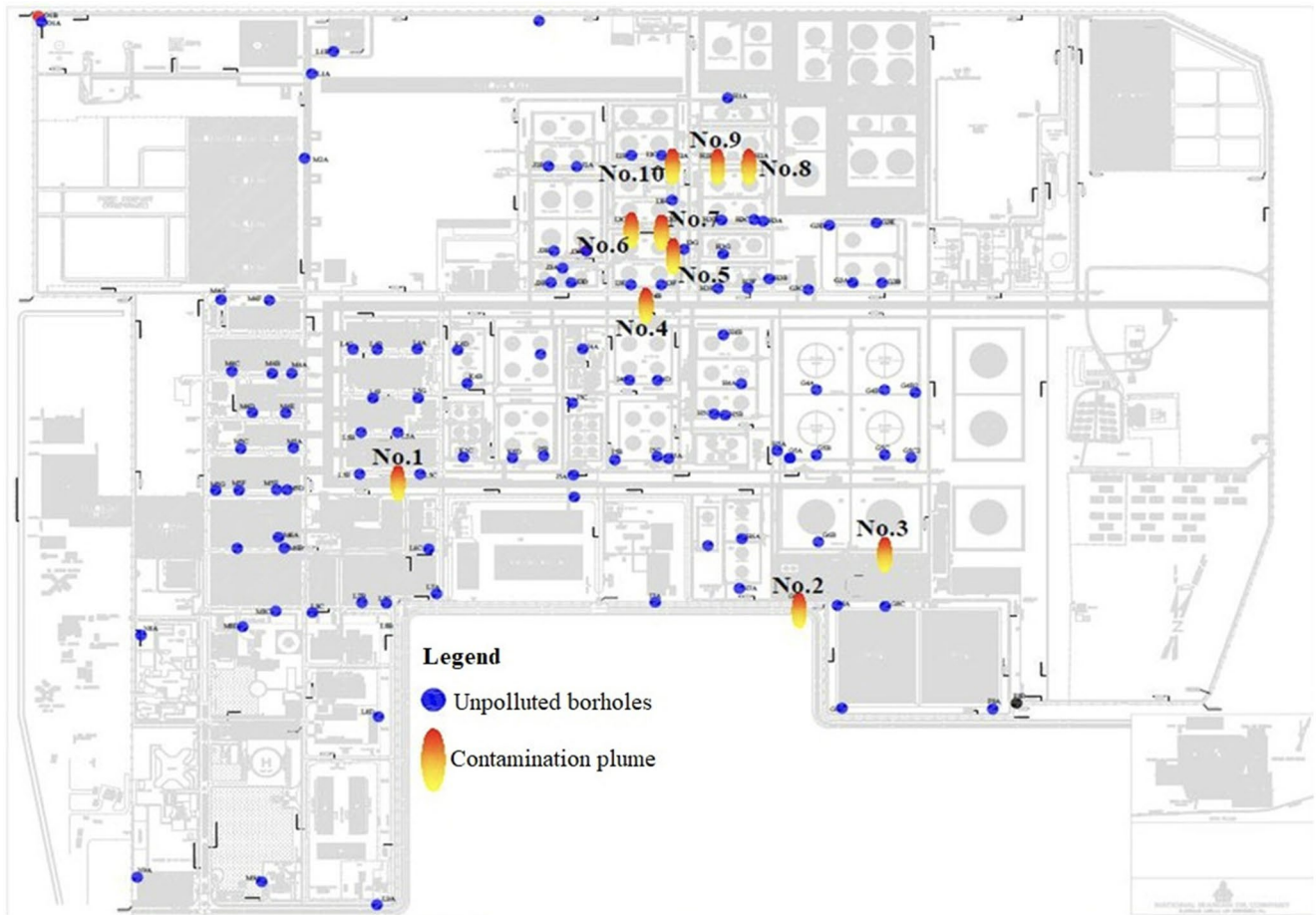
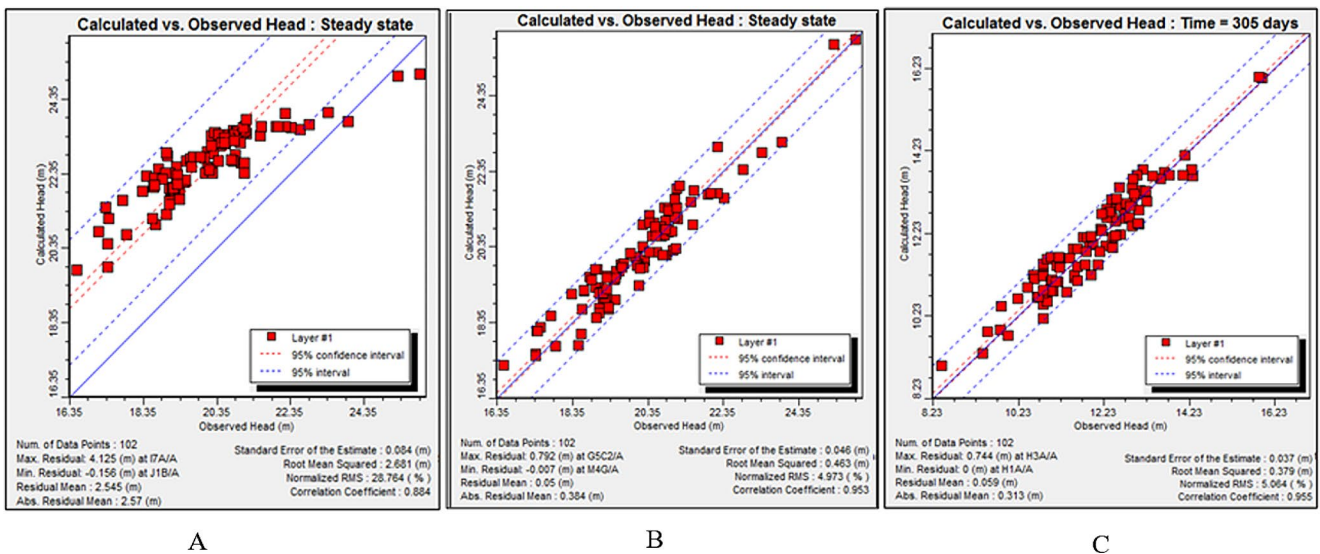**Fig. 4** Location of LNAPL masses identified on site

Fig. 5 **A**: Residual analysis of calculated and observations hydraulic head in steady state at the first run of the model (before calibration), **B**: Residual analysis of calculated and observed head in steady state (after calibration), **C**: Calculated and observed head during the verification stage

This required interpreting all available findings about the aquifer, contaminants, and historical leak information. By considering these factors, it was found that oil processing

unit 71 is the main suspected source for the first plume around well L5D.

Flow and transport modeling

Groundwater flow modeling

The output data from the simulation indicated a moderate fit and coincidence between simulated and observed data (Fig. 5A). In this step, metrics to evaluate the model performance including the route mean square, standard error, and correlation coefficient were estimated to be 2.68 m, 28.76%, and 0.88, respectively.

To decrease the bias between the simulated and observed data, it was necessary to calibrate input parameters to their actual value. Before calibration, considering the uncertainty of parameters, a sensitivity analysis was conducted to investigate the response of the model to any changes in parameters value. The results of sensitivity analysis showed the highest sensitivity of the model to the hydraulic head in the

Table 3 Parameters and values used for sensitivity analysis of the transport model

Parameter	Value	Plume extension (m)	Change percent (%)
Concentration (mg/L)	890	350	5.71
	1780	370	0
	2670	400	7.5
Longitudinal dispersivity (m)	5	310	19.35
	10*	370	0
	15	430	10.81
Hydraulic Conductivity (m/d)	3.67	450	18.8
	2.45*	370	0
	1.22	290	27.6
Distribution Coefficient (K_d)(mg/L)	6.75×10^{-8}	410	9.75
	1.35×10^{-7}	370	0
	2.02×10^{-7}	35	5.71

boundaries of the model. Evaporation has the least effect on the groundwater flow, with the minimum sensitivity (see Table A.2 in the supplementary file).
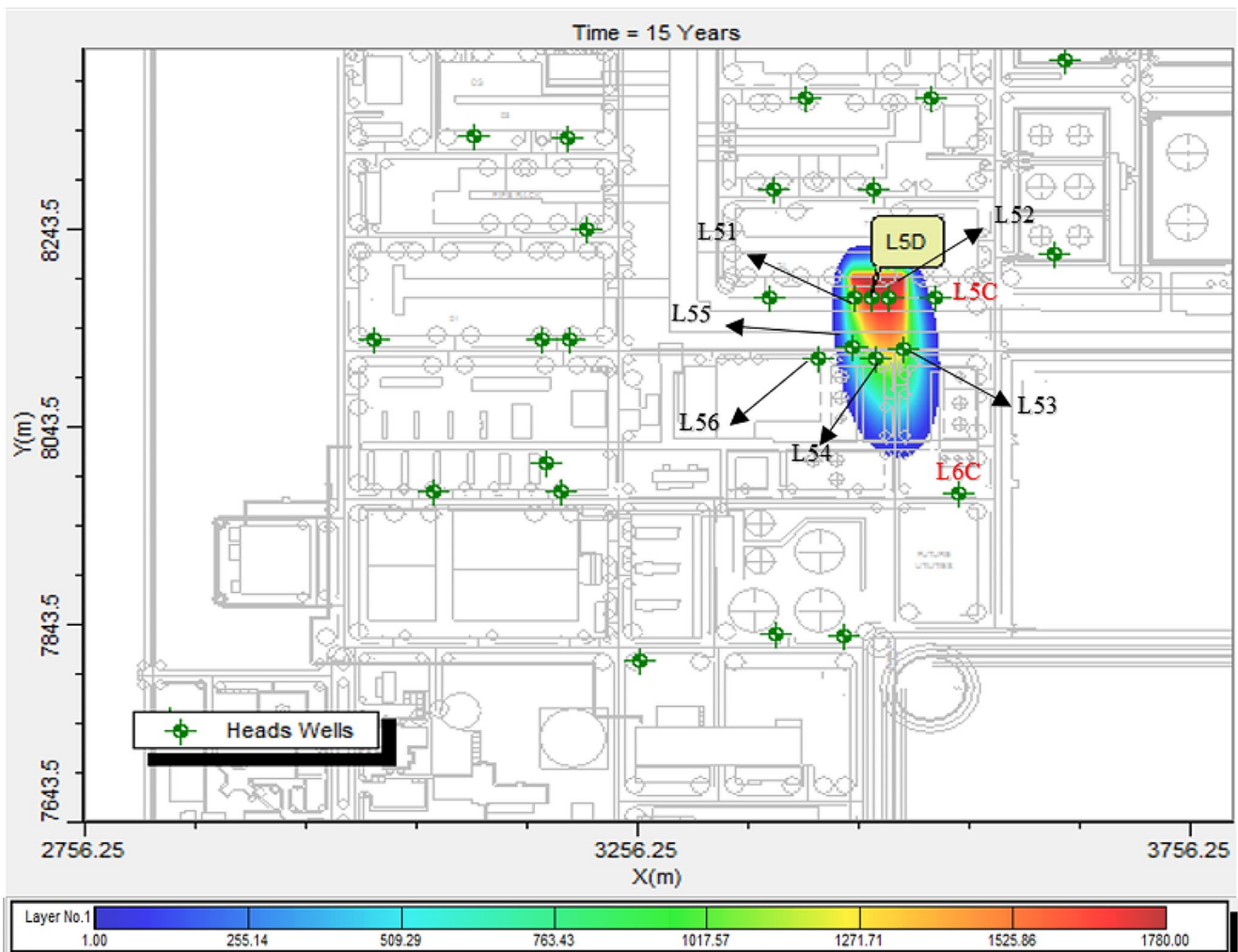
**Fig. 6** Plume distribution (leakage beginning in the year 2001)

Calibration of the model was carried out by focusing on the sensitive parameters (hydraulic conductivity of boundaries). The calibration process continued until an acceptable error value between simulated and observed data (Fig. 5B). As a result, the route mean square, standard error, and correlation coefficient decreased to 0.46 m, 4.97%, and 0.95, respectively, indicating an acceptable correlation between simulated and observed data. Moreover, the groundwater flow model was run for unsteady conditions using monthly stress periods and daily time steps. Parameter calibration was also performed for the unsteady condition to minimize error. To ensure the accuracy of the model, another run was carried out for unsteady conditions to predict the condition of the aquifer in September 2018. The results (Fig. 5C) confirmed that the model is verified and can accurately predict the state of the aquifer.

Table 4 Remediation scenarios

Parameter	Sorption	Source of leak	LNAPL Remediation	BTEX Remediation
First scenario	√	Continuous	Without remediation	Without remediation
Second scenario	✗	Continuous	Without remediation	Without remediation
Third scenario	√	Interrupted in 2018	Without remediation	Without remediation
Fourth scenario	√	Interrupted in 2018	Remediation of mass in 2021	Without remediation
Fifth scenario	√	Interrupted in 2018	Remediation of 50% of the mass in 2021	Remediation of 50% of BTEX in 2021

Mass Transport modeling

In the second part of the modeling, the mass transport simulation was conjugated with the verified flow model, and the transport model was developed by employing MT3D/MS.
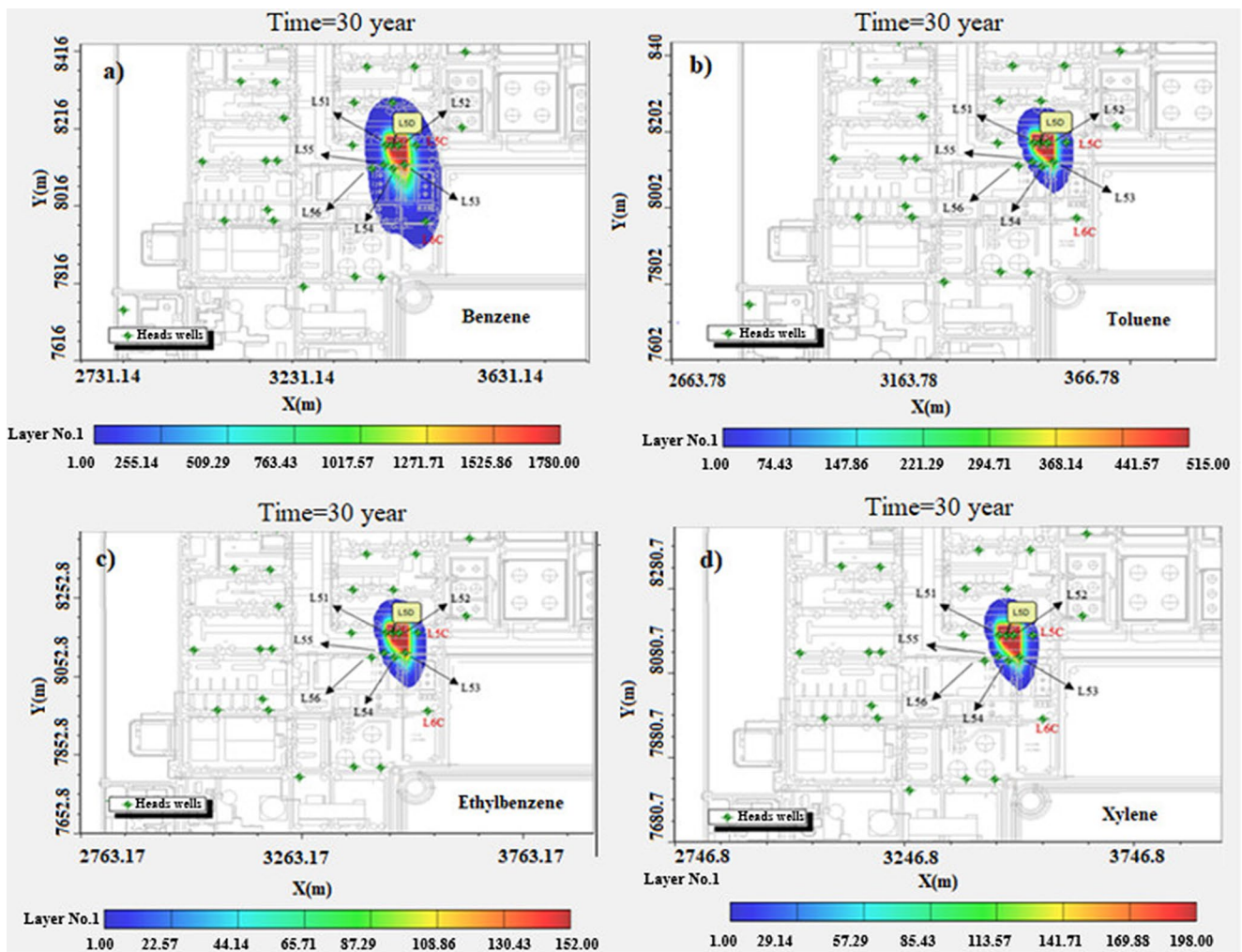
Fig. 7 Simulated plume for **a**) benzene **b**) Toluene, **c**) ethyl benzene, and **d**) xylene 30 years after the beginning of leakage (first scenario)
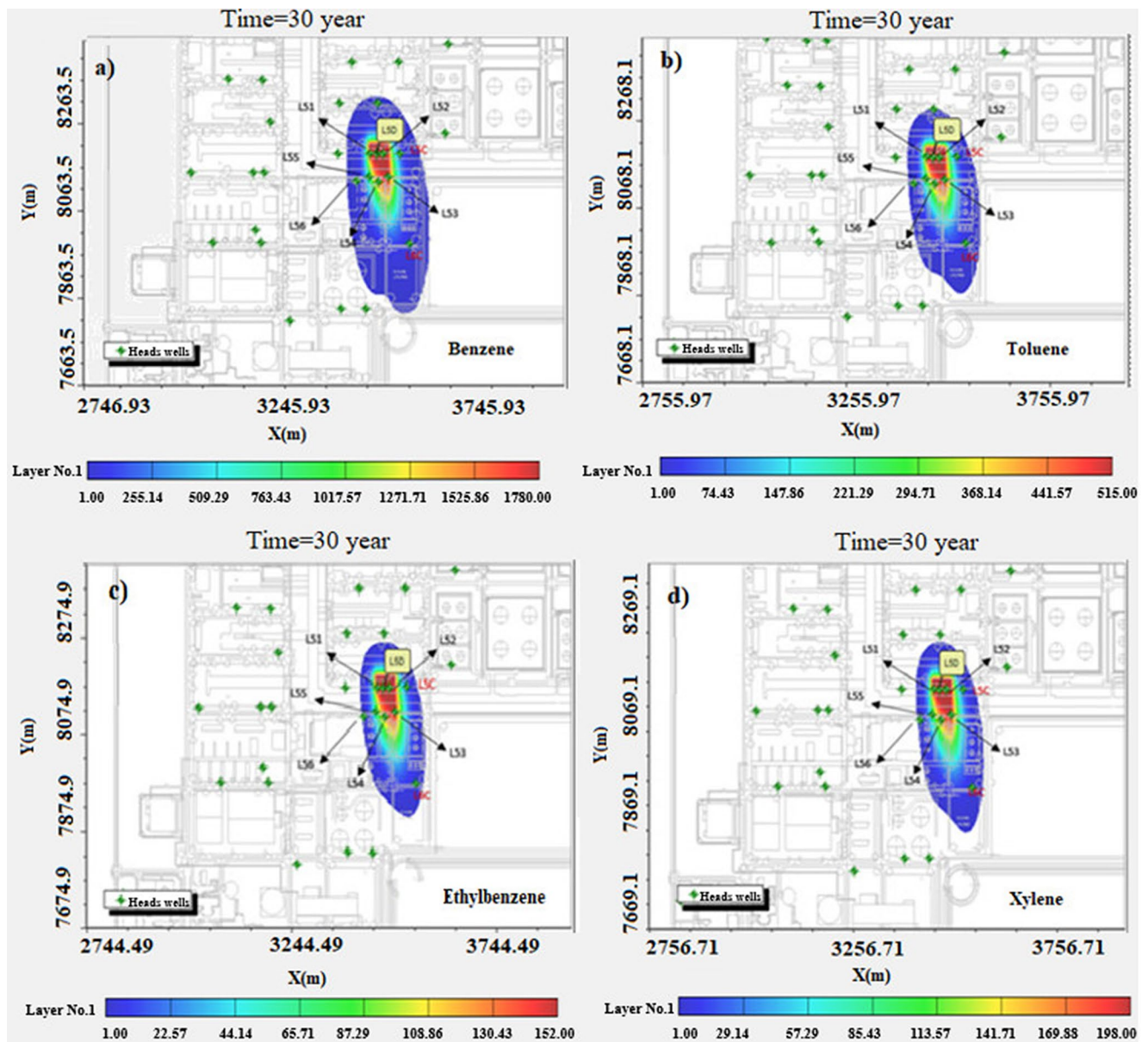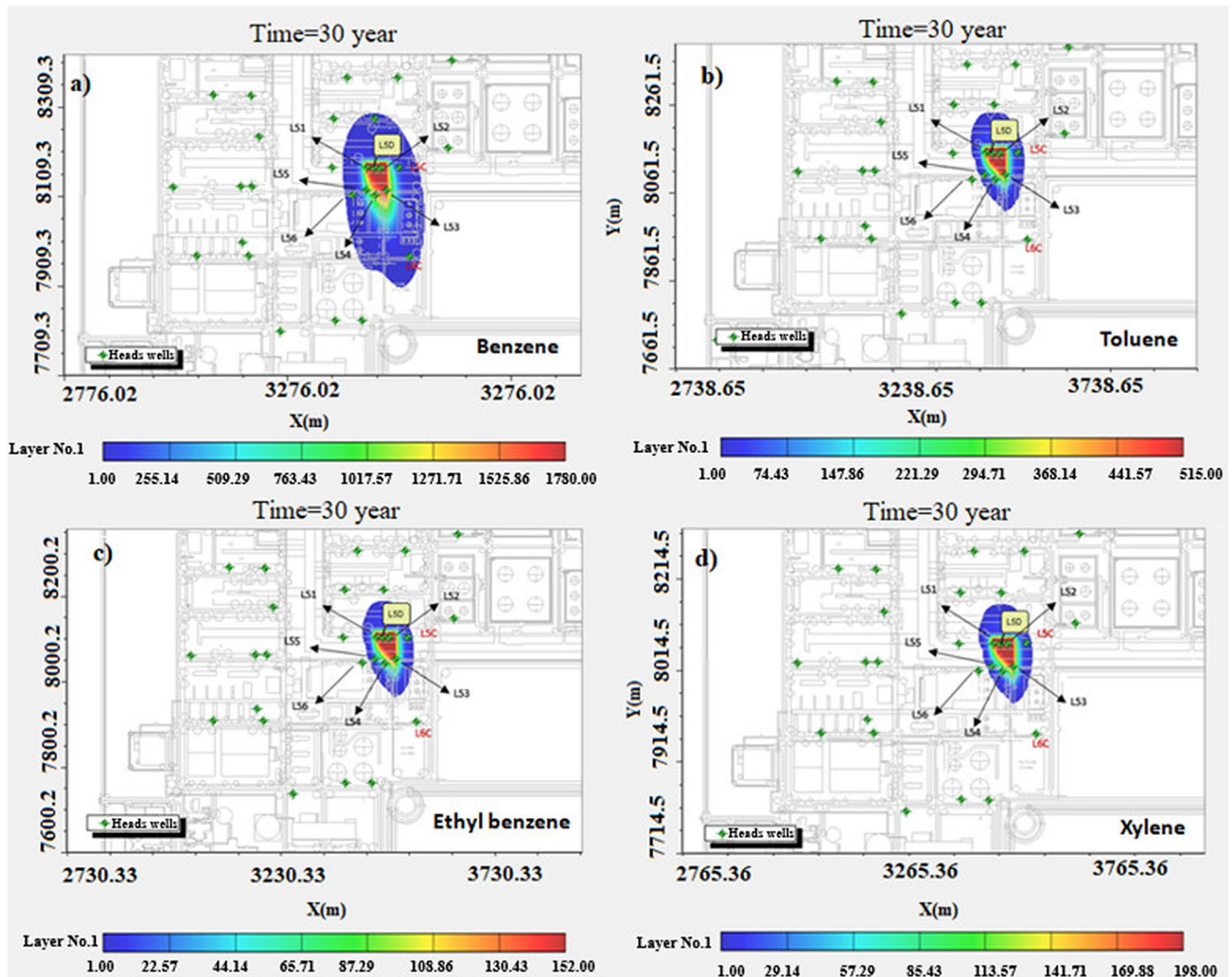
Fig. 8 Simulated plumes: **a**) benzene, **b**) toluene **c**) ethyl benzene, and **d**) xylene 30 years after the beginning of leakage (second scenario**)**

To satisfy Pecelet and Courant's criteria, the mesh (cell) size of the discretized model was decreased to 10×10 m with telescopic finer cells relative to the flow model. Various transport parameters that were entered into the model have been summarized in Table 2.

For sorption isotherm a linear relationship was assumed with a distribution coefficient adopted from EPA (US EPA 1990). It was also assumed that there was no reaction between the contaminant and the media. The initial condition for the mass transport modeling was set based on the date of contamination leakage. Since the exact date of leakage was not determined, the first overhaul date of the refinery in 2001 was assigned as the initial time of modeling.

As mentioned previously, plume number 1, originating from LNAPL (light non-aqueous phase liquid) with crude oil as the source, was selected for transport modeling. This plume had contaminated the groundwater downstream of unit 71 at the refinery. The dimensions of LNAPL were determined to be 3270 m^2 with a thickness of 1.30 m, which releases BTEX as a dissolved phase into groundwater. The boundary condition for the transport model was set with no mass inflow from any of the boundaries. The contaminant entered the model only from a specified cell located in the north of the area. Finally, the south boundary was regarded as a mass outflow boundary. Hence, after the initial running of the model in steady conditions, a sensitivity analysis

Fig. 9 Simulated plume for **a**) benzene, **b**) toluene, **c**) ethyl benzene, and **d**) xylene 30 years after the beginning of leakage

was carried out for the main parameters as a pre-required step of the calibration. The result of the sensitivity analysis (Table 3) revealed that the model is most sensitive to hydraulic conductivity and longitudinal dispersivity while being less sensitive to contaminant concentration.

The results of the water sample analysis were used to compare the observed concentrations with the simulated data. Based on the model results for the initial plume, the current condition, 17 years after leakage, indicated that the benzene plume had dimension of 200×80 m, which was confirmed by observed concentration data. To predict the fate of the plume under various conditions, five scenarios were defined according to the condition of the source leak, sorption, and contaminant remediation. All scenarios were run for the duration of 30 and 50 years from the leakage date for all BTEX compounds. The simulated plume length obtained from this scenario was 200 m, which corresponds

to field observations and hydrocarbon analysis of the wells in the area (Fig. 6).

Remediation scenarios

To evaluate the distribution and expansion of contaminants in the aquifer and examine the effect of various scenarios, including with or without the leakage source, the contamination transport modeling was implemented in the five scenarios for periods of 30 and 50 years from 2001 to 2051. The results of 50-year periods have been shown in the supplementary file, Figs. A.6 to A.10. Five scenarios were considered based on the various remediation strategies to predict the contamination behavior under different remediation conditions (Table 4).
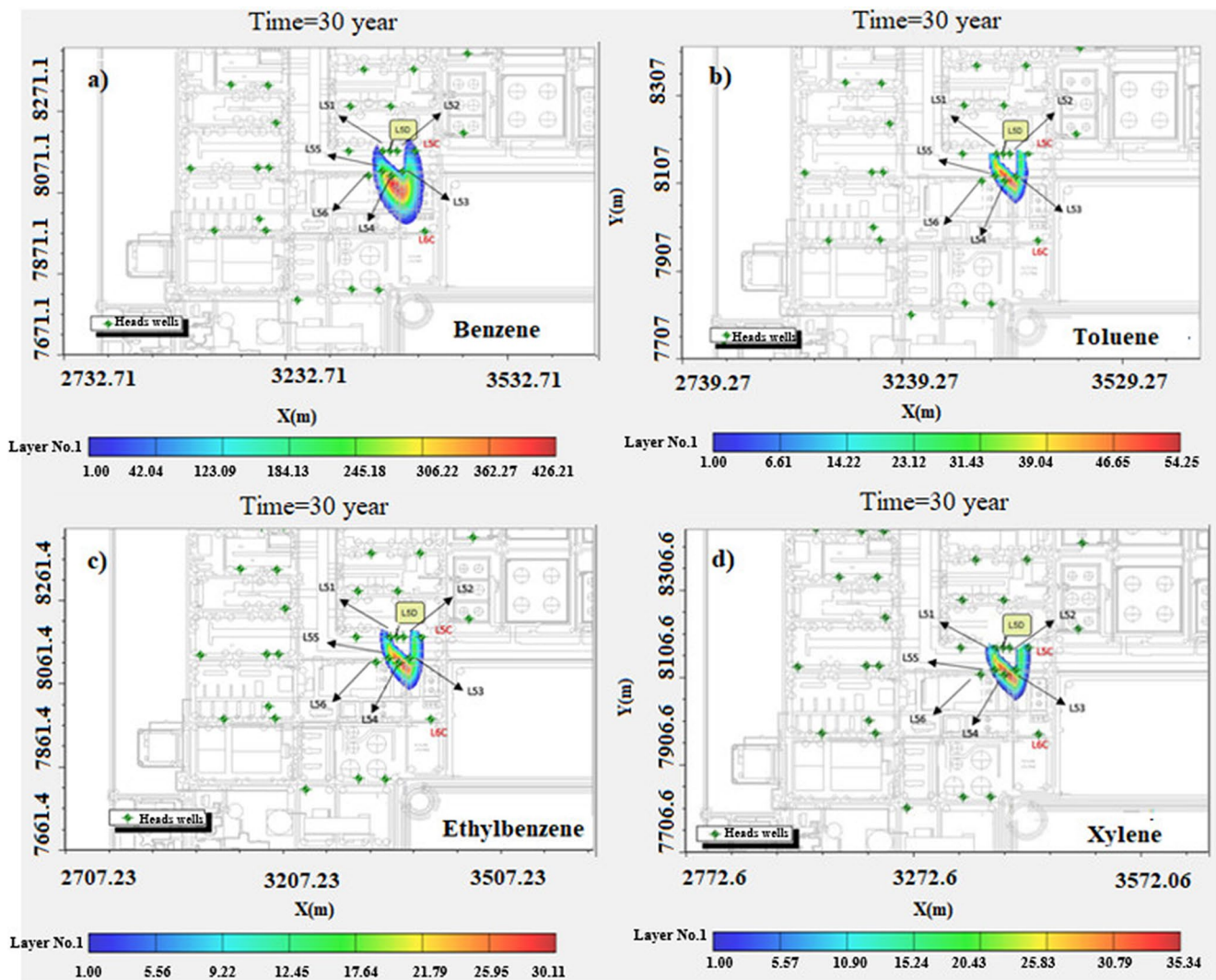
Fig. 10 Simulated Plume for **a**) benzene, **b**) toluene, **c**) ethyl benzene, and **d**) xylene 30 years after the beginning of leakage (fourth scenario)

First Scenario (Base case scenario)

In this scenario, the contamination leakage from the source is continuous, meaning that the contamination release rate is constant. However, the contamination movement is affected by the sorption process. The result of this scenario for the transport of BTEX is presented in Fig. 7. According to the first scenario, assuming the leakage started in the year 2001, the distribution of plumes for benzene, toluene, ethyl benzene, and xylene after 30 years (in the year 2031) are 370, 200, 220 and 200 m, respectively. The results of this scenario are consistent with findings in wells L53, L54, L55, and L4C, which are contaminated by BTEX compounds. Similarly, benzene reached well L56 with a concentration of about 10 mg/L and well L6C with a concentration of about 50 mg/L.

Based on the results of this scenario, 50 years after the beginning of leakage (the year 2051) the BTEX plume spread over a significant distance of 470, 250, 270, and 250 m, respectively. Also, the results suggested that the highest concentration of BTEX is observed in well L53, with increasing concentrations in wells L54 and L55. The monitoring well L5C is also contaminated. In addition, the contaminant benzene would reach well L56 with a concentration of about 50 mg/L, contaminate well L6C downstream, and reach the southern border of the refinery with a concentration of 1 mg/L.

Second scenario (worst case scenario)

In this scenario, the leakage is continuous and the concentrations are constant during the simulation period; also, the sorption parameter is considered zero. These results (Fig. 8) show that 30 years after the first contaminant leakage (in the year 2031), the extension of BTEX plumes would be 430, 400, 350, and 370 m, respectively. Moreover, the simulation
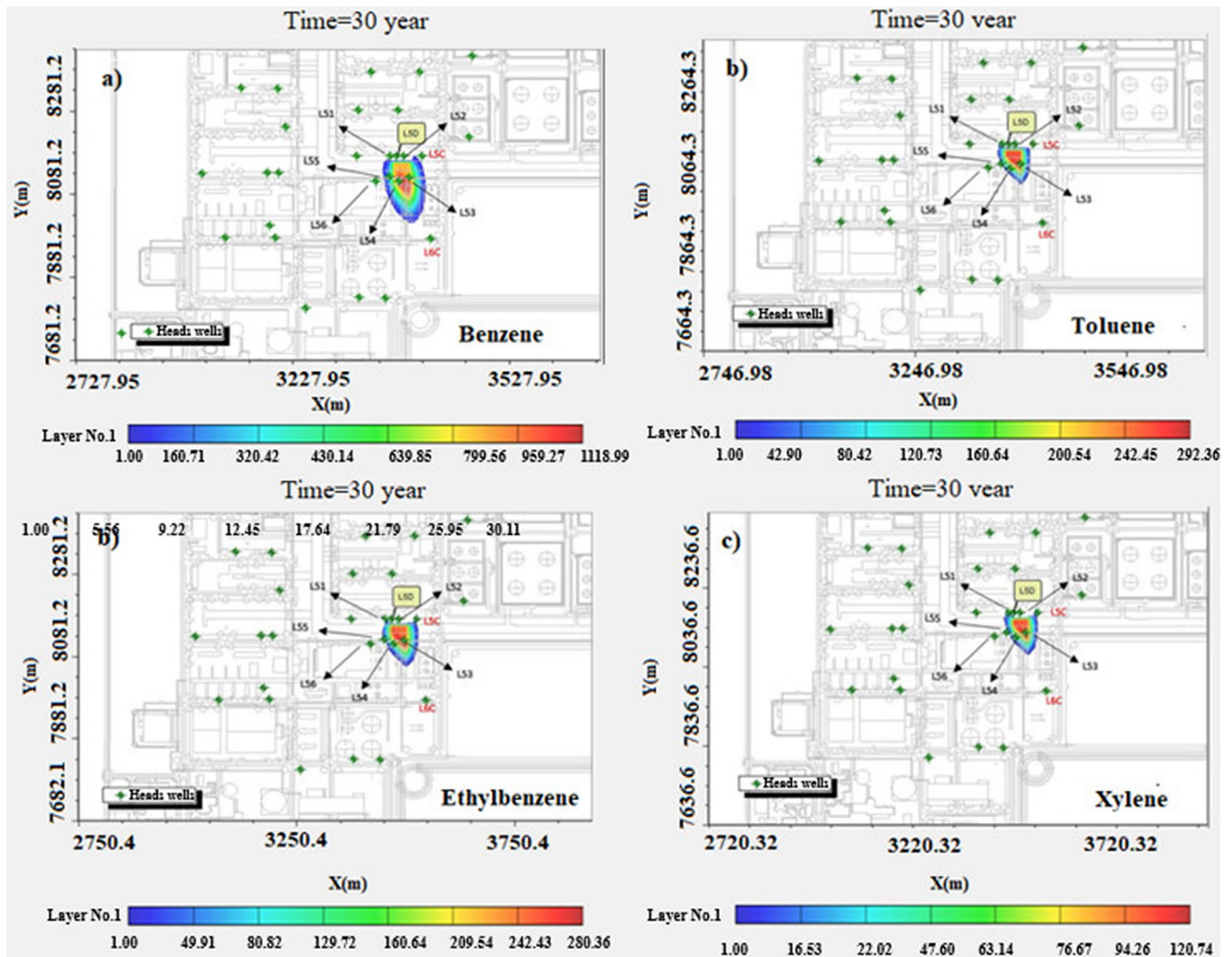
Fig. 11 Simulated Plume: **a**) benzene, **b**) toluene, **c**) ethyl benzene, and **d**) xylene 30 years after the beginning of the leak (fifth scenario)

results represent the monitoring wells of L53, L54, L55, and L5C would be contaminated with BTEX compounds and benzene would contaminate wells L56 and L6C downstream with a concentration of about 100 mg/L. After 30 years, the benzene plume is predicted to reach the south border of the refinery.

Additionally, after 50 years (in the year 2051), the BTEX plume extension would be 480, 450, 400, and 420 m, respectively. The results suggest that the maximum BTEX concentration would be observed in well L53 and increased in monitoring wells L54 and L55. In addition, the contaminants would reach well L56 with a concentration of about 130 mg/L. The plume is also anticipated to reach the drain channel located at the south border of the refinery.

The third scenario (non-continuous source without remediation)

Based on this scenario, the contamination source is non-continuous and is removed 15 years after the beginning of the leakage (the year 2016). In this scenario, the sorption process affects the movement of the contaminants and is executed in the simulation. This scenario determines how the contaminant expansion behaves if the contamination source was cut off 15 years after the beginning of the leak. The results showed that under this condition, the contamination plume of BTEX compounds would expand about 350, 200, 220, and 200 m from the source, respectively. The results revealed that only benzene contaminant would reach wells L56 and L6C downstream of the source (Fig. 9).

The fourth scenario (non-continuous source and removing of LNAPL, optimistic scenario)

In this scenario, similar to the third one, the source is non-continuous, and it is removed 15 years after the beginning of the leakage in 2001. The LNAPL completely is removed and the sorption process is active during the simulation. From 2016 to 2021, LNAPL mass would be presented and by 2021 contamination concentration decrease to 1 mg/L. Under the mentioned conditions, after 30 years from the leakage beginning, the plume of BTEX compounds is up to 1 mg/L at distances of 150, 70, 90, and 80 m, respectively. Furthermore, the monitoring wells L51, L5D, and L52 are reported to be without contaminants. However, wells L53 and L5C remain contaminated, while wells L55 and L54 represent the maximum contamination of BTEX compounds. Thus, during this period the contamination would not reach the monitoring wells L56 and L6C downstream (Fig. 10).

Transport modeling in this scenario for 50 years from the leakage time showed that the plumes of benzene, toluene, ethylbenzene, and xylenes will reach 180, 80, 100, and 90 m downstream, respectively. This scenario results in the complete remediation in wells L51, L5D, and L52 due to the plume detachment from the source. Concentration in wells L53 and L5C decreased to 1 mg/L, while wells L54 and L55 have the maximum contamination due to the movement of the plume. An important point to note is that only the benzene plume has reached well L6C According to the results, in this scenario, the remediation process has the potential to progress towards complete remediation and inhibit migration of the plume to reach the downstream wells and south border of the refinery.

Fifth scenario (non-continuous source and removing 50% of LNAPL, realistic scenario)

Based on this scenario the contamination source is non-continuous, the leakage is cut off after 15 years (from the beginning of the leak in 2001) in 2016, LNAPL is removed up to 50% and the sorption process is actively occurring during the simulation. From the year 2016 to 2021, the LNAPL mass caused by the leak source is present in the area. In 2021, 50% of this LNAPL will be removed, then the concentration of BTEX compounds will be reduced to 50%. According to the result, 30 years from the beginning of the leak, the BTEX plumes are projected to extend to distances of approximately 180, 80, 100, and 90 m, respectively. The wells L51, L5D, L52, L5C, and L56 are reported to be contamination-free and the concentration of benzene in wells L53 and L54 is projected to reach 750 mg/L (Fig. 11).

The simulated plume extent for periods of 30 and 50 years in the five scenarios has been summarized in Table 5. The velocity of plume movement for benzene contamination in the base scenario was calculated to be 0.03 m/day.

Conclusion

Based on pumping test results, the hydraulic conductivity, transmissivity, and groundwater velocity of the aquifer were determined to be 2.45 m/ day, 24.5 m²/ day, and 0.02 m/ day, respectively. The model has revealed the most sensitivity to changes in the hydraulic head at the boundaries. While the model has minor sensitivity to evaporation. The results of the second scenario, where continuous leakage is considered and the absorption is neglected, revealed that the spread of the plume is estimated to be 15% higher compared to the first scenario.

The results of the third scenario, with a non-continuous source and adsorption process indicated that the BTEX will continue to spread even after 30 years and 50 years. However, the remediation process can prevent the spread of contamination from reaching the southern border. In scenario 4, by cutting off the leakage source after 15 years and, with an active absorption and completely removing LNAPL (light non-aqueous phase liquid), after 5 years the pollution was reduced to 1 mg/l. It greatly prevents the spread of pollution to the downstream wells and the southern border of the refinery. Applying the last scenario, where similar to the fourth scenario but removing LNAPL by 50%, the result indicated that After 30 years, it is predicted that the downstream section will be free of contamination and the concentration of benzene will reach approximately 750 mg/L. Also, simulation of the model for 50 years from the beginning time of leakage revealed that the benzene plume will reach downstream. The findings of this research highlight the importance of absorption processes and effective remediation

Table 5 Plume expansions of BTEX under different scenarios

	30 years of simulation				50 years of simulation			
	B	T	E	X	B	T	E	X
Scenario 1	370	200	220	200	470	250	270	**250**
Scenario 2	430	400	350	370	480	450	400	**420**
Scenario 3	350	200	220	200	450	220	240	**220**
Scenario 4	150	70	90	80	210	100	120	**100**
Scenario 5	180	80	100	90	230	120	150	**150**

strategies to mitigate contamination in the aquifer and suggest that the implementation of remediation measures can effectively reduce pollution and prevent its further spread. However, long-term monitoring and ongoing remedial efforts may be required to prevent the contamination downstream area or to completely remove it from affected areas.

Declarations

Competing interests The authors declare that they have no known competing financial interests or personal relationships that could have appeared to influence the work reported in this paper.

References

Ahmadnezhad Z, Vaezihir A, Schüth C, Zarrini G (2021) Combination of zeolite barrier and bio sparging techniques to enhance efficiency of organic hydrocarbon remediation in a model of shallow groundwater. Chemosphere no 273:128555. https://doi.org/10.1016/j.chemosphere.2020.128555

Anderson MP, Woessner WW, Hunt RJ (2015) Applied groundwater modeling: simulation of flow and advective transport. Academic

Ayvaz MT (2016) A hybrid simulation–optimization approach for solving the areal groundwater pollution source identification problems. J Hydrology no 538:161–176. https://doi.org/10.1016/j.jhydrol.2016.04.008

Babaei M, Copty NK (2019) Numerical modelling of the impact of surfactant partitioning on surfactant-enhanced aquifer remediation. J Contaminant Hydrology no 221:69–81. https://doi.org/10.1016/j.jconhyd.2019.01.004

Badv K, Seyyedi BM, Nimtaj A (2020) Numerical Investigation of Propagation of BTEX compounds in Soil. Geotech Geol Eng 38:4: 3875–3890. https://doi.org/10.1007/s10706-020-01263-z

Bai X, Song K, Liu J, Mohamed AK, Mou C, Liu D (2019) Health risk assessment of groundwater contaminated by oil pollutants based on numerical modeling. Int J Environ Res Public Health 16:18: 3245. https://doi.org/10.3390/ijerph16183245

Batu V (2005) Applied flow and solute transport modeling in aquifers: fundamental principles and analytical and numerical methods. CRC

Bayatian M, Ashrafi K, Azari MR, Jafari MJ, Mehrabi Y (2018) Risk assessment of occupational exposure to benzene using numerical simulation in a complex geometry of a reforming unit of petroleum refinery. Environ Sci Pollut Res 25(12):11364–11375. https://doi.org/10.1007/s11356-018-1318-6

Bedekar V (2019) Development, Numerical Implementation, and Application of Methods to Simulate Solute Transport Processes in Porous Media Systems

Cheng Y, Chen Y, Jiang Y, Jiang L, Sun L, Li L, Huang J (2016) Migration of BTEX and biodegradation in shallow underground water through fuel leak simulation. *BioMed research international*. 2016

Ciampi P, Esposito C, Cassiani G, Deidda GP, Rizzetto P, Papini MP (2021) A field-scale remediation of residual light non-aqueous phase liquid (LNAPL): chemical enhancers for pump and treat. Environ Sci Pollut Res 28(26):35286–35296

Davis GB, Barber C, Power TR, Thierrin J, Patterson BM, Rayner JL, Wu Q (1999) The variability and intrinsic remediation of a BTEX plume in anaerobic sulphate-rich groundwater. J Contam Hydrol 36(3–4):265–290. https://doi.org/10.1016/S0169-7722(98)00148-X

De Martonne E (1926) Une nouvelle fonction climatologique:L'indice d'aridite᷄. La Meteorol, pp 449–458

Demenev A, Maksimovich N, Khmurchik V, Rogovskiy G, Rogovskiy A, Baryshnikov A (2022) Field test of in situ groundwater treatment applying oxygen diffusion and bioaugmentation methods in an area with sustained total petroleum hydrocarbon (TPH) contaminant flow. Water 14(2):192. https://doi.org/10.3390/w14020192

Essaid HI, Bekins BA (1997) BIOMOC, a multispecies solute-transport model with biodegradation (Vol. 97, No. 4022). US Department of the Interior, US Geological Survey

Feng Y, Xiao A, Jia R, Zhu S, Gao S, Li B, … and, Zou B (2020) Emission characteristics and associated assessment of volatile organic compounds from process units in a refinery. Environ Pollution no 265:115026. https://doi.org/10.1016/j.envpol.2020.115026

Ghosh S, Patra R, Majumdar D, Sen K (2020) Developing scenario of titania-based building materials for environmental remediation. Int J Environ Sci Technol 1–26. https://doi.org/10.1007/s13762-020-02952-1

Guarnaccia J, Pinder G, Fishman M (1997) NAPL: simulator documentation ((EPA/600/R-97/102)). National Risk Management Research Laboratory Ada, Oklahoma, United States Environmental Protection Agency, Research and Development

Guiguer T, Franz N (1994) User's Manual of Visual MODFLOW V.3.1. Waterloo Hydro geologic. Inc. Canada

Hamamin D (2018) F. Passive soil gas technique for investigating soil and groundwater plume emanating from volatile organic hydrocarbon at Bazian oil refinery site. *Science of the Total Environment*. no, 622:1485–1498. https://doi.org/10.1016/j.scitotenv.2017.11.328

He L, Huang GH, Lu HW (2009) A coupled simulation-optimization approach for groundwater remediation design under uncertainty: an application to a petroleum-contaminated site. Environ Pollut 157:8–9. https://doi.org/10.1016/j.envpol.2009.03.005

Ismail RE, Al-Raoush RI, Alazaiza MY (2023) The impact of water table fluctuation and salinity on LNAPL distribution and geochemical properties in the smear zone under completely anaerobic conditions. Environ Earth Sci 82(15):368. https://doi.org/10.1007/s12665-023-11051-6

Leili M, Farjadfard S, Sorial GA, Ramavandi B (2017) Simultaneous biofiltration of BTEX and hg from a petrochemical waste stream. J Environ Manage no. 204:531–539. https://doi.org/10.1016/j.jenvman.2017.09.033

Molson JW (2017) BIONAPL/3D user guide: a 3D Groundwater Flow, and multi- component NAPL dissolution with dissolved-phase advective- dispersive transport and biodegradation. Porous and fractured porous media. University of Waterloo, Waterloo, pp 1–89

Neuman SP (1975) Analysis of pumping test data from anisotropic unconfined aquifers considering delayed gravity response. Water Resour Res 11(2):329–342

O'Connor D, Hou D, Ok YS, Song Y, Sarmah AK, Li X, Tack FM (2018) Sustainable in situ remediation of recalcitrant organic pollutants in groundwater with controlled release materials: a review. J Controlled Release no 283:200–213. https://doi.org/10.1016/j.jconrel.2018.06.007

Pal S, Banat F, Almansoori A, Abu Haija M (2016) Review of technologies for biotreatment of refinery wastewaters: progress, challenges and future opportunities. Environ Technol Reviews 5(1):12–38. https://doi.org/10.1080/21622515.2016.1164252

Palma E, Tofalos AE, Daghio M, Franzetti A, Tsiota P, Viggi CC, … and, Aulenta F (2019) Bioelectrochemical treatment of groundwater containing BTEX in a continuous-flow system: substrate interactions, microbial community analysis, and impact of sulfate as a co-contaminant. New Biotechnol no 53:41–48. https://doi.org/10.1016/j.nbt.2019.06.004

Rama F, Ramos DT, Müller JB, Corseuil HX, Miotliński K (2019) Flow field dynamics and high ethanol content in gasohol blends enhance BTEX migration and biodegradation in groundwater. J Contaminant Hydrology no 222:17–30. https://doi.org/10.1016/j.jconhyd.2019.01.003

Ramezanzadeh M, Aminnaji M, Rezanezhad F, Ghazanfari MH, Babaei M (2022) Dissolution and remobilization of NAPL in surfactant-enhanced aquifer remediation from microscopic scale simulations. Chemosphere 289:133177. https://doi.org/10.1016/j.chemosphere.2021.133177

Rifai HS, Newell CJ, Gonzales JR, Dendrou S, Kennedy L, Wilson JT (1997) BIOPLUME III natural attenuation decision support system, version 1.0, user's manual, Air Force Cent. Environ. Excell. (AFCEE), San Antonio

Sathe SS, Mahanta C (2019) Groundwater flow and arsenic contamination transport modeling for a multi aquifer terrain: Assessment and mitigation strategies. J Environ Manage no 231:166–181. https://doi.org/10.1016/j.jenvman.2018.08.057

Schirmer M, Molson JW, Frind EO, Barker JF (2000) Biodegradation modelling of a dissolved gasoline plume applying independent laboratory and field parameters. J Contam Hydrol 46(3–4):339–374

Seyedpour SM, Kirmizakis P, Brennan P, Doherty R, Ricken T (2019) Optimal remediation design and simulation of groundwater flow coupled to contaminant transport using genetic algorithm and radial point collocation method (RPCM). Sci Total Environ no 669:389–399. https://doi.org/10.1016/j.scitotenv.2019.01.409

Shafieiyoun S, Al-Raoush RI, Ngueleu SK, Rezanezhad F, Van Cappellen P (2020) Enhancement of naphthalene degradation by a sequential sulfate injection scenario in a (Semi)-Arid coastal soil: a flow-through reactor experiment 231. 81–16. https://doi.org/10.1007/s11270-020-04725-5

Sharma MK, Jain CK, Rao GT, Rao VG (2015) Modelling of lindane transport in groundwater of metropolitan city Vadodara, Gujarat, India. Environ Monit Assess 187(5):1–19. https://doi.org/10.1007/s10661-015-4522-6

Srivastav A, Yadav KK, Yadav S, Gupta N, Singh JK, Katiyar R, Kumar V (2018) Nano-phytoremediation of pollutants from contaminated soil environment: current scenario and future prospects. *In Phytoremediation* (pp. 383–401). Springer, Cham

Steiner LV, Ramos DT, Liedke AMR, Serbent MP, Corseuil HX (2018) Ethanol content in different gasohol blend spills influences the decision-making on remediation technologies. J Environ Manage no 212:8–16. https://doi.org/10.1016/j.jenvman.2018.01.071

Talbot CJ, Alavi M (1996) The past of a future syntaxis across the Zagros. Geological Society, London, Special Publications 100, no. 1: 89–109., https://doi.org/10.1144/GSL.SP.1996.100.01.08

Talbot C, Aftabi P, Chemia Z (2009) Potash in a salt mushroom at Hormoz Island, Hormoz Strait, Iran. Ore Geol Rev 35:3–4. https://doi.org/10.1016/j.oregeorev.2008.11.005

Teramoto EH, Chang HK (2020) A screening model to predict entrapped LNAPL depletion. Water 12(2):334. https://doi.org/10.3390/w12020334

Todd DK, Mays LW (2005) Groundwater hydrology edition. Third edit, vol 891. John Wiley & Sons, Inc.

USEPA (EPA) (1990) CERCLA site discharges to POTWS: Treatability manual. EPA Washington, DC

Vaezihir A, Zare M, Raeisi E, Molson J, Barker J (2012) Field-scale modeling of benzene, toluene, ethylbenzene, and xylenes (BTEX) released from multiple source zones. Bioremediat J 16(3):156–176. https://doi.org/10.1080/10889868.2012.687415

Vaezihir A, Zare M, Barker J, Grathwohl P, Raeisi E (2013) Source determination for subsurface light non-aqueous phase liquid (LNAPL) using trimethylcyclopentane and trimethylcyclohexane isomer ratios. Environ Forensics 14(1):25–35. https://doi.org/10.1080/15275922.2012.760177

Vaezihir A, Bayanlou MB, Ahmadnezhad Z, Barzegari G (2020) Remediation of BTEX plume in a continuous flow model using zeolite-PRB. J Contaminant Hydrology no 230:103604. https://doi.org/10.1016/j.jconhyd.2020.103604

Vaezihir A, Mohammadzadeh Motlaq M, Bakhtiari S, Nematollahi R (2021) Identification of LNAPL phase of oil contaminants in the aquifer of Bandar Abbas Oil Refinery. J Human Environ 19(4:59):141–158. SID. https://sid.ir/paper/1043092/en [In Persian]

Valsala R, Govindarajan SK (2018) Mathematical modeling on mobility and spreading of BTEX in a discretely fractured aquifer system under the coupled effect of dissolution, sorption, and biodegradation. Transp Porous Media 123(2):421–452. https://doi.org/10.1007/s11242-018-1049-7

Valsala R, Govindarajan SK (2019) Co-colloidal BTEX and microbial transport in a saturated porous system: numerical modeling and sensitivity analysis. Transp Porous Media 127(2):269–294. https://doi.org/10.1007/s11242-018-1191-2

Wang Y (2020) Aquifer Experiments for Characterizing NAPL Sources and Dissolved Plumes following Releases of Ethanol-Blended Fuels (Doctoral dissertation, University of Houston)

Wiedemeier TH, Rifai HS, Newell CJ, Wilson JT (1999) Natural attenuation of fuels and chlorinated solvents in the subsurface. John Wiley & Sons

Zanello V, Scherger LE, Lexow C (2021) Assessment of groundwater contamination risk by BTEX from residual fuel soil phase. SN Appl Sci 3(3):307